Assistive technology: autonomous wheelchair in obstacle-ridden environment

Sandeep Ameet Kumar, Jito Vanualailai and Avinesh Prasad

School of Information Technology, Engineering, Mathematics, and Physics, The University of the South Pacific, Suva, Fiji

ABSTRACT

The benefits for the advancement and enhancement of assistive technology are manifold. However, improving accessibility for persons with disabilities (PWD) to ensure their social and economic inclusion makes up one of the major ones in recent times. This paper presents a set of new nonlinear time-invariant stabilizing controllers for safe navigation of an autonomous nonholonomic rear-wheel drive wheelchair. Autonomous wheelchairs belong to the category of assistive technology, which is most sought in current times due to its usefulness, especially to the less abled (physically and/or cognitively), hence helping create an inclusive society. The wheelchair navigates in an obstacle-ridden environment from its start to final configuration, maintaining a robust obstacle avoidance scheme and observing system restrictions and dynamics. The velocity-based controllers are extracted from a Lyapunov function, the total potentials designed using the Lyapunov based Control Scheme (LbCS) falling under the classical approach of the artificial potential field method. The interplay of the three central pillars of LbCS, which are safety, shortness, and smoothest course for motion planning, results in cost and time effectiveness and the velocity controllers' efficiency. Using the Direct Method of Lyapunov, the stability of the wheelchair system has been proved. Finally, computer simulations illustrate the effectiveness of the set of new controllers.

INTRODUCTION

Information and Communications Technologies (ICT) has shaped the global transformation into information societies since the late 20th century. ICT is continuing to evolve with the introduction of newer, more enhanced, sophisticated, and targeted technologies. ICT tools have become an indispensable component of everyday life and for every human endeavor. Most sectors, such as socio-economic, political, educational, medical, and healthcare sectors, are integrating innovative ICT tools developed by the industries to their systems and processes to secure solutions tailored to their needs. The inclusion of wireless and sensor technologies have resulted in improved and new designs of assistive technologies. According to the Individuals with Disabilities Education Act (2019), assistive technology device refers to "any item, piece of equipment, or product system, whether acquired commercially off the shelf, modified, or customized, that is used to increase, maintain, or improve functional capabilities of a child with a disability".

Corresponding author
Sandeep Ameet Kumar,
sandeep.a.kumar@usp.ac.fj

These assistive technologies allow people with severe paralysis to interact and communicate with other industry developed devices such as television set, radio, computer, laptop, and tablets. The objective is to extend the remaining abilities of a person living with severe disabilities to perform limited activities (*Moon, Baker & Goughnour, 2019*; *Assaf et al., 2018*; *Utkal, Mohammed & Shivneel, 2017*). For those having physical debility, mobility is a luxury for them. It is an issue for those who have walking disabilities, such as the elderly, physically disabled, and weak medical care patients. The wheelchair is one of the most frequently used assistive technology in recent and past decades to aid mobility for people with walking disabilities (*Borges et al., 2018*). Consequentially, a high degree of research work has been in progress to design user-friendly, collision-free electrical and smart wheelchairs such as joystick controlled (*Hartman & Nandikolla, 2019*), smartphone controlled (*Borges et al., 2018*; *Gulpanich, Petchhan & Wongvanich, 2018*), gesture controlled (eye movement (*Solea et al., 2015*; *Bharath, Sreenidhi & Tarun, 2018*; *Eid, Giakoumidis & Saddik, 2016*; *Maule et al., 2016*), oral motion (*Saitoh, Takahashi & Konishi, 2007*), and head motion (*Tomari, Kobayashi & Kuno, 2014*)), voice controlled (*Chen et al., 2008*), brain controlled (*Xin et al., 2018*; *Ng & Goh, 2020*), blue-tooth controlled (*Qin, Li & Nawaz, 2018*), multiple control interfaces (*Yashoda et al., 2018*; *Shahnaz et al., 2017*), and semi-autonomous controlled (*Tomari, Kobayashi & Kuno, 2012*) to improve mobility, which can enhance the quality of life for the elderly and the disabled (*Takahashi & Murakami, 2018*; *Bumuller & Skerl, 2018*; *Chen et al., 2008*). The design of wheelchairs has to be such that the safety and comfortability of its users should not be compromised, rather enhanced (*Tomari, Kobayashi & Kuno, 2014*). It should also uplift the lifestyle of its users in terms of social interactions, access to education and opportunities, and the ability to exercise their knowledge and skills (*Shahnaz et al., 2017*). While wheelchairs have been most sought for mobility, integration of ICTs and controller laws are gradually transforming these assistive vehicles into smart, intelligent or autonomous robots. Futuristic models seek to be independent of controls that require human interaction, and transform them into fully automated systems. For instance, those suffering from severe motor impairment face difficulties in operating electric or smart wheelchairs that require user input or interaction (*Assaf et al., 2018*; *Tomari, Kobayashi & Kuno, 2012*) will prefer automated wheelchairs instead. Electronic and smart wheelchairs (*Assaf et al., 2018*; *Borges et al., 2018*; *Hartman & Nandikolla, 2019*; *Gulpanich, Petchhan & Wongvanich, 2018*; *Solea et al., 2015*; *Bharath, Sreenidhi & Tarun, 2018*; *Eid, Giakoumidis & Saddik, 2016*; *Maule et al., 2016*; *Saitoh, Takahashi & Konishi, 2007*; *Tomari, Kobayashi & Kuno, 2014*; *Chen et al., 2008*; *Xin et al., 2018*; *Ng & Goh, 2020*; *Qin, Li & Nawaz, 2018*; *Yashoda et al., 2018*; *Shahnaz et al., 2017*; *Tomari, Kobayashi & Kuno, 2012*; *Takahashi & Murakami, 2018*; *Bumuller & Skerl, 2018*; *Chen et al., 2008*) present in the literature are mostly experimental types, and the stability of these systems are missing together with robust control laws which can make these robots fully autonomous. Recently, *Andaluz et al. (2015)* and *Herrera et al. (2018)* presented the kinematic and dynamic modeling of a human-wheelchair system which is capable of performing positioning and path-following tasks in a shared environment. Moreover, using the path following control laws, the notion of

graceful motion, that is, the movement that is safe, smooth, fast, and intuitive, for a robotic wheelchair presented in *Gulati & Kuipers (2008)* concentrated on a specific task of narrow way clearance. An assistive collision avoidance method developed in *Gillham & Howells (2015)* based on potential fields required human interaction for a powered wheelchair that allows the user to navigate safely.

In this paper, a set of new nonlinear time invariant stabilizing velocity-based controllers is developed which facilitates navigation of an autonomous wheelchair robot in an obstacle-ridden environment, maintaining a robust obstacle avoidance scheme and observing system restrictions and dynamics. Stabilizing controllers are derived from a total potential function developed using the Lyapunov based Control Scheme (LbCS) which has been deployed successfully in literature to find feasible and stabilizing solutions for a wide spectrum of applications (*Sharma, Vanualailai & Singh, 2012*; *Sharma, Vanualailai & Singh, 2014*; *Kumar, Vanualailai & Sharma, 2015a*; *Kumar et al., 2016*; *Devi et al., 2017*; *Sharma, Vanualailai & Singh, 2015*; *Sharma, Raj & Vanualailai, 2018*; *Sharma, Vanualailai & Prasad, 2017*; *Sharma et al., 2018*; *Raghuwaiya, Sharma & Vanualailai, 2018*; *Sharma, Vanualailai & Prasad, 2011*; *Kumar, Vanualailai & Sharma, 2015b*; *Kumar & Vanualailai, 2017*; *Kumar et al., 2021b*; *Prasad et al., 2020*). Interaction of the three main pillars of LbCS, which are safety, shortness, and smoothest path for motion planning, bring about cost and time effectiveness and efficiency of the velocity controllers. From the authors' viewpoint, this is the first instance the methodology is applied to wheelchairs.

The major contributions of this paper are:

1. Design of a set of new stabilizing nonlinear time-invariant continuous controllers for an autonomous wheelchair robot for navigation observing system restrictions and limitations through the use of LbCS. From the authors' point of view, this is the first time such stabilizing continuous velocity-based controllers are derived for autonomous wheelchairs in the sense of Lyapunov. Similar obstacle avoidance scheme was presented in *Rösmann, Hoffmann & Bertram (2017)*, however, using inequalities, whereas in *Darweesh et al. (2017)*, planning and tracking are split, and the mechanical singularities and constraints are not considered within the path planner. Similarly, *Lazarowska (2019)* does not consider the mechanical singularities and constraints despite of effective solutions in terms of the path length and run time of the algorithm.

2. Obstacle avoidance in an environment without any interaction between the user and the wheelchair. In contrast, the wheelchairs reported in the literature mostly require human interaction for it to be able to reach the rider's destination safely. Wheelchairs that require human interaction could collide with obstacles as weak motor patients sometimes would not be able to react on time. For instance, while controlling button-based, voice-based (*Gulpanich, Petchhan & Wongvanich, 2018*; *Chen et al., 2008*; *Qin, Li & Nawaz, 2018*; *Yashoda et al., 2018*; *Shahnaz et al., 2017*), head movement-based (*Borges et al., 2018*; *Tomari, Kobayashi & Kuno, 2014*), oral motion controlled (*Saitoh, Takahashi & Konishi, 2007*), joystick-based (*Borges et al., 2018*; *Yashoda et al., 2018*), eyeball sensed (*Borges et al., 2018*; *Solea et al., 2015*; *Eid, Giakoumidis & Saddik, 2016*;

Maule et al., 2016) and EEG signaled (*Xin et al., 2018*; *Ng & Goh, 2020*) wheelchairs. Moreover, the wheelchairs, such as the ones reported in references (*Borges et al., 2018*; *Gulpanich, Petchhan & Wongvanich, 2018*; *Solea et al., 2015*; *Eid, Giakoumidis & Saddik, 2016*; *Maule et al., 2016*; *Saitoh, Takahashi & Konishi, 2007*; *Tomari, Kobayashi & Kuno, 2014*; *Chen et al., 2008*; *Xin et al., 2018*; *Ng & Goh, 2020*; *Qin, Li & Nawaz, 2018*; *Yashoda et al., 2018*; *Shahnaz et al., 2017*; *Tomari, Kobayashi & Kuno, 2012*), that require human interactions cannot perform the simplest of the tasks of moving from one place to the other for persons with special disabilities who are incapable of any interactions or cannot provide any commands to the wheelchairs.

3. Optimal route amidst obstacles, constraints and restrictions from start to target points inherently guaranteed by the LbCS.

 The remainder of the paper is organized as follows: "Lyapunov-Based Control Scheme" gives a brief description of the LbCS. In "Kinematic Model of a Nonholonomic Wheelchair", kinematic equations of a rear two wheels driven wheelchair robot with two front castor wheels based on a geometric model are developed assuming there is no lateral slip motion on the wheels, and there is pure rolling. "Velocity Controllers of the Wheelchair Robot", the nonlinear time-invariant stabilizing velocity controllers are derived for the wheelchair robot using LbCS. In "Angular Velocities and their Limitations", the restrictions on the angular velocities of the wheels of the wheelchair robot are discussed. The stability analysis of the wheelchair robot system is presented in "Stability Analysis". The simulation studies are presented in "Simulation Results". Finally, a discussion on the results presented is provided in "Discussion" and the research is concluded with a brief on future undertakings in "Conclusion".

LYAPUNOV-BASED CONTROL SCHEME

This research utilizes an artificial potential field technique known as the Lyapunov-based control scheme. The development of attractive and repulsive potential field functions is the primary intention of LbCS. Subsequently, these functions are part of a total potential function called the Lyapunov function from which one could extract the time-invariant nonlinear velocity or acceleration controllers (*Sharma, Vanualailai & Singh, 2014*; *Sharma, Vanualailai & Singh, 2015*; *Sharma, Raj & Vanualailai, 2018*; *Sharma, Vanualailai & Prasad, 2017*; *Sharma et al., 2018*; *Kumar et al., 2021b*; *Prasad et al., 2020*; *Chand et al., 2020*; *Prasad et al., 2021*; *Kumar et al., 2021a*). Using LbCS, designing controllers is easy, and the controllers are continuous, which are its strength. It is easy to include control conditions, specifications, inequalities, and mechanical constraints of mechanical systems in the controllers through developing mathematical functions when applying LbCS. The main disadvantage of LbCS is that algorithm singularities (local minima) can be introduced. In practical applications, continuity has to be discretized, and only then asymptotic stability could be shown. The reader is referred to *Sharma, Vanualailai & Singh (2014)* and *Sharma, Vanualailai & Prasad (2017)* for a detailed account of the LbCS.
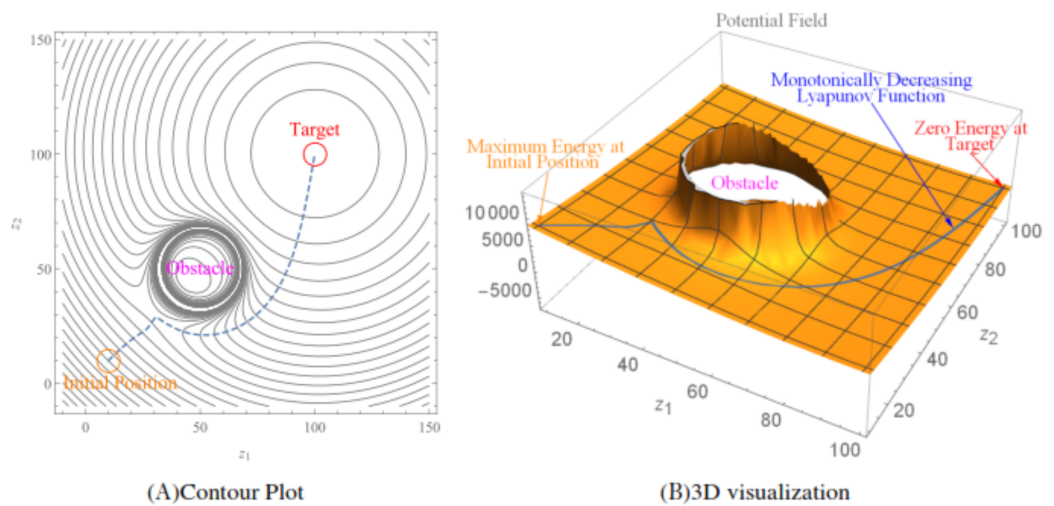
Figure 1 An illustration of the Lyapunov-based control scheme.

An illustration of the LbCS is given utilizing Figs. 1A and 1B. Figure 1A shows the contour plot generated over a workspace:amp:minus; $-10 < z_2 < 150$ and $-10 < z_1 < 150$ for a robot whose initial position is at $(10, 10)$. The dashed line is the robot's trajectory from its initial position to its target position $(100, 100)$, which shows the robot avoids the obstacle positioned at $(50, 50)$ with radius 10. Figure 1B shows the 3D visualization of the attractive and repulsive potential fields. The blue line shows the Lyapunov function, which shows that the energy of the robot is monotonically decreasing and is zero at the target position.

KINEMATIC MODEL OF A NONHOLONOMIC WHEELCHAIR

Definition 3.1 A rear two wheels driven wheelchair with two front castor wheels is a disk with radius r_w and is positioned at center (x, y). A wheelchair is precisely described as the set

$$V = \{(z_1, z_2) \in \mathbb{R}^2 : (z_1 - x)^2 + (z_2 - y)^2 \le r_w^2\}. \tag{1}$$

A two rear wheels driven wheelchair robot with two front castor wheels is shown in Fig. 2. The two rear drive wheels of radius r are on opposite ends of a wheelbase of length ς. The angle θ is the orientational angle of the wheelchair robot with respect to z_1-axis of the $z_1 z_2$ cartesian plane. The centre of the wheelchair robot is at (x, y) which is at a distance of η with orientational angle θ from the centre of the two rear diametrically opposed wheels. The angular velocities of the rear right and left wheels are $\dot{\phi}_R = v_R$ and $\dot{\phi}_L = v_L$, respectively. To ensure that the wheelchair robot steers safely pass obstacles (either moving or static obstacles), the wheelchair is enclosed by a smallest possible circle. As shown in Fig. 2, the wheelchair robot is enclosed by a protective circular region centered at (x, y), with radius $r_w := \sqrt{\left(\frac{\varsigma}{2}\right)^2 + (\eta + r)^2}$. Hence, the configuration vector for the wheelchair robot is,
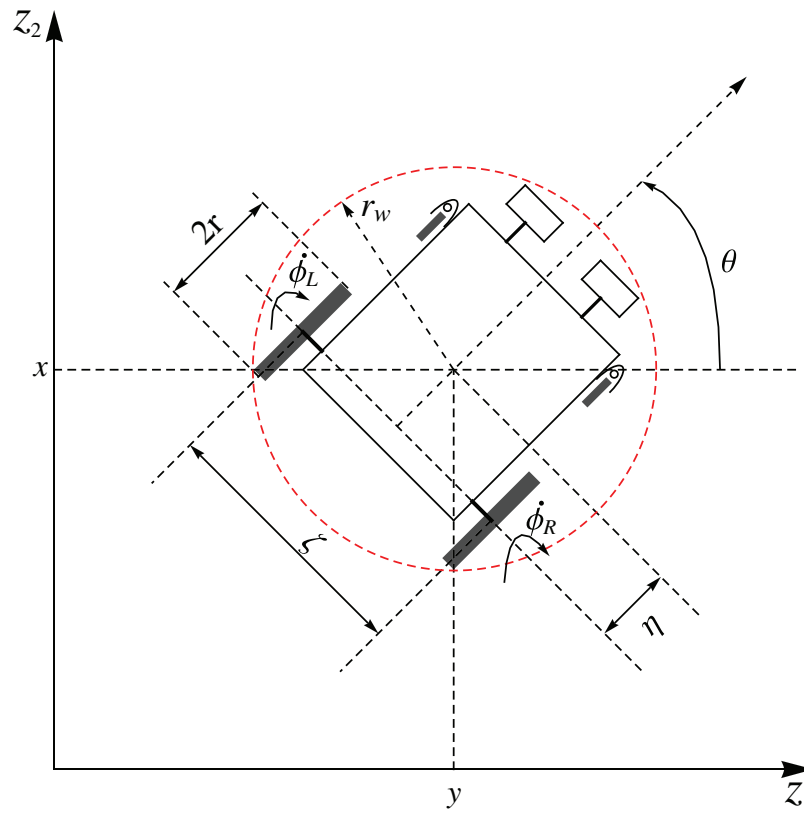
Figure 2 Geometric model of a two rear wheels driven wheelchair with two front castor wheels at an orientational angle θ.

$$\mathbf{q} = [x, y, \theta, \phi_R, \phi_L]. \tag{2}$$

It has been assumed that there are no uncertainties in the kinematic parameters of the wheel radius and the wheelbase. Moreover, assuming that there is pure rolling and no lateral slip motion on the two rear wheels, with respect to (x, y) the following constraints are obtained:

$$\dot{y}\cos\theta - \dot{x}\sin\theta - \dot{\theta}\eta = 0 \tag{3}$$

$$\dot{x}\cos\theta + \dot{y}\sin\theta + \frac{\zeta}{2}\dot{\theta} - r\dot{\phi}_R = 0 \tag{4}$$

$$\dot{x}\cos\theta + \dot{y}\sin\theta - \frac{\zeta}{2}\dot{\theta} - r\dot{\phi}_L = 0. \tag{5}$$

This is in line with the derivations obtained in the literature by *Solea et al. (2015)* and *Dhaouadi & Hatab (2013)*. These are the non-holonomic constraints of the wheelchair robot which needs to be appropriately factored into the kinematic model of the robot. The kinematic model, of the robot with respect to its center $(x, y) \in \mathbb{R}^2$ is derived as

$$\left.\begin{aligned}
\dot{x} &= \frac{r}{\zeta}\left(v_R\left(\frac{\zeta}{2}\cos\theta - \eta\sin\theta\right) + v_L\left(\frac{\zeta}{2}\cos\theta + \eta\sin\theta\right)\right), \\
\dot{y} &= \frac{r}{\zeta}\left(v_R\left(\frac{\zeta}{2}\sin\theta + \eta\cos\theta\right) + v_L\left(\frac{\zeta}{2}\sin\theta - \eta\cos\theta\right)\right), \\
\dot{\theta} &= \frac{r}{\zeta}(v_R - v_L), \\
\dot{\phi}_R &= v_R, \\
\dot{\phi}_L &= v_L.
\end{aligned}\right\} \tag{6}$$

In a two-dimensional space, the position of a wheelchair robot can be described by its translational components. Let the position of a wheelchair at time $t \geq 0$ be $\mathbf{x} = (x(t), y(t))$ and orientational angle $\theta = \theta(t)$, with $(x(t_0), y(t_0)) =: (x_0, y_0)$ and $\theta(t_0) = \theta_0$ as initial conditions. At $t \geq 0$, let $(\rho(t), \omega(t)) := (x'(t), y'(t))$ be the instantaneous velocity of the wheelchair robot. We have thus a system of first-order ODEs for the wheelchair robot:

$$x'(t) = \rho(t), \quad y'(t) = \omega(t), \tag{7}$$

assuming the initial conditions at $t = t_0 \geq 0$ as $x_0 := x(t_0), \; y_0 := y(t_0))$. Suppressing t, we let $\mathbf{x} := (x, y) \in \mathbb{R}^2$ and let $\mathbf{x}_0 := \mathbf{x}(t_0) := (x_0, y_0) \in \mathbb{R}^2$. If the instantaneous velocity (ρ, ω) has a state feedback law of the form

$$\rho(t) := -\mu f(\mathbf{x}(t)),$$
$$\omega(t) := -\varphi g(\mathbf{x}(t)),$$

for some scalars $\mu, \varphi > 0$ and some functions $f(\mathbf{x}(t))$ and $g(\mathbf{x}(t))$ to be constructed appropriately later, and if we define $\mathbf{G}(\mathbf{x}) := (-\mu f(\mathbf{x}), -\varphi g(\mathbf{x})) \in \mathbb{R}^2$, then the wheelchair robot is represented by

$$\underline{\mathbf{x}} = \mathbf{G}(\mathbf{x}), \quad \mathbf{x}(t_0) = \mathbf{x}_0. \tag{8}$$

The equilibrium point for the wheelchair robot is $\mathbf{x}_e = (x_e, y_e) \in \mathbb{R}^2$.

VELOCITY CONTROLLERS OF THE WHEELCHAIR ROBOT

Consider *a priori* known workspace cluttered with $q \in \mathbb{N}$ stationary obstacles. The wheelchair robot governed by system (8) has to maneuver to its target, avoiding collision with static obstacles.

Definition 4.1 The kth solid stationary obstacle is a disk with center $\mathbf{x}_{O_k} = (o_{k1}, o_{k2})$ and radius $r_{O_k} > 0$. It is described as the set

$$O_k := \{(z_1, z_2) \in \mathbb{R}^2 : (z_1 - o_{k1})^2 + (z_2 - o_{k2})^2 \leq r_{O_k}^2\}. \tag{9}$$

Definition 4.2 The target for the wheelchair robot is $\mathbf{x}_\tau$. It is a disk with center $\mathbf{x}_\tau = (a, b)$ and radius r_w. It is described as the set

$$\tau := \{(z_1, z_2) \in \mathbb{R}^2 : (z_1 - a)^2 + (z_2 - b)^2 \leq r_w^2\}. \tag{10}$$
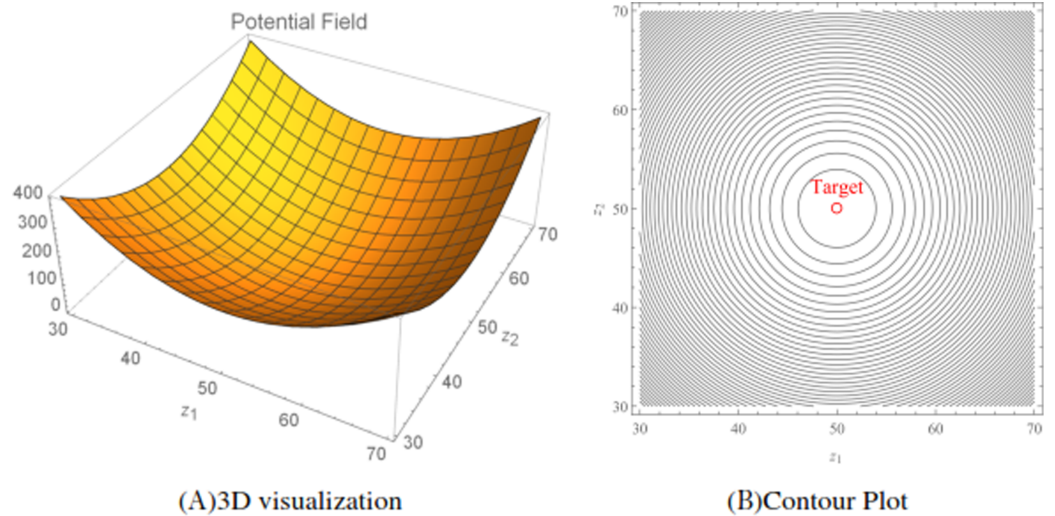
Figure 3 The attractive potential fields and the corresponding contour plot generated using the attractive potential function (11). The position of the target is located at (50, 50) with a $r_w = 0.5$. The target convergence parameter $\alpha = 1$.

Components of the Lyapunov function

In the Lyapunov function to be proposed for the total potential, the following attractive and repulsive potential functions will be included.

Target attraction

To ensure that the wheelchair robot converges to its equilibrium position, we shall utilize the target attraction potential function

$$U_{att}(\mathbf{x}) := \frac{1}{2}\alpha \mathbf{e}_1{}^2, \tag{11}$$

where $\alpha > 0$ is the target convergence parameter, and $\mathbf{e}_1 = \|\mathbf{x} - x_\tau\|$ is the distance between the wheelchair robot position and the target at any arbitrary time. The target convergence parameter, α, can be considered as a measurement of the strength of attraction between the wheelchair robot, $\mathbf{x}$, and its target, $\mathbf{x}_\tau$. A small value of the parameter indicates a slower convergence of the wheelchair robot to its target. An illustration of the total potentials for the function (11) is shown in Fig. 3A, while Fig. 3B shows the corresponding contour plot generated over a workspace $30 < z_1 < 70$ and $30 < z_2 < 70$.

Stationary obstacle avoidance

For the purpose of avoiding possible collisions with the kth stationary solid obstacle governed by Eq. (9), the following obstacle avoidance function will be utilized for the wheelchair robot:

$$W_k(\mathbf{x}) = \frac{1}{2}\left[\mathbf{e}_2{}^2 - (r_{O_k} + r_w)^2\right], \quad k \in \{1, 2, \dots, q\}. \tag{12}$$

(A)3D visualization   (B)Contour Plot
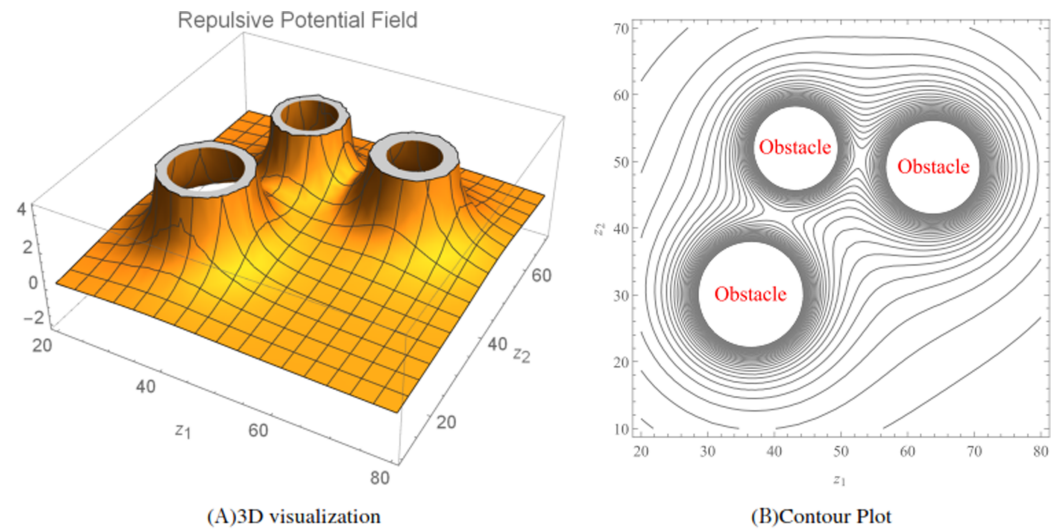
Figure 4 The repulsive potential fields and the corresponding contour plot generated using the repulsive potential function (13). The radius of the obstacles were randomized between three and five and $r_w = 1$. The obstacle avoidance parameter β_k for $k = 1, 2$ and 3 were randomized between 30 and 70.

where $\mathbf{e}_2 = \|\mathbf{x} - \mathbf{x}_{O_k}\|$ is the distance between the wheelchair robot position and the centre of the obstacle at any arbitrary time. Thus, the total repulsive potential is given by

$$U_{rep}(\mathbf{x}) = \sum_{k=1}^{q} \frac{\beta_k}{W_k(\mathbf{x})} \tag{13}$$

where $\beta_k > 0$ is the obstacle avoidance parameter. At large distances between the wheelchair robot and the kth obstacles, ratio (13) is negligible. Now, consider the situation where the wheelchair robot approaches the kth obstacle. In this case, $W_k(\mathbf{x})$ decreases, and the ratio (13) increases, with $\beta_k > 0$ acting as a *obstacle avoidance parameters*, that is a measurement of the strength of interaction between the wheelchair robot and the kth obstacle. Here, the ratio (13) acts as an *collision-avoidance function* because it can be allowed to increase in value (corresponding to avoidance) as the wheelchair robot approaches the stationary obstacle. An illustration of the total repulsive potentials for three randomly generated obstacles ($q = 3$) for the function (13) is shown in Fig. 4A, while Fig. 4B shows the corresponding contour plot generated over a workspace $20 < z_1 < 80$ and $10 < z_2 < 70$.

Auxiliary function
To ensure that the wheelchair robot converges to its target and guarantee that the nonlinear velocity controllers vanish at the target consider the auxiliary function of the form

$$H(\mathbf{x}) := \frac{1}{2}\mathbf{e}_1^2 \tag{14}$$

PeerJ Computer Science

(A)3D visualization   (B)Contour Plot
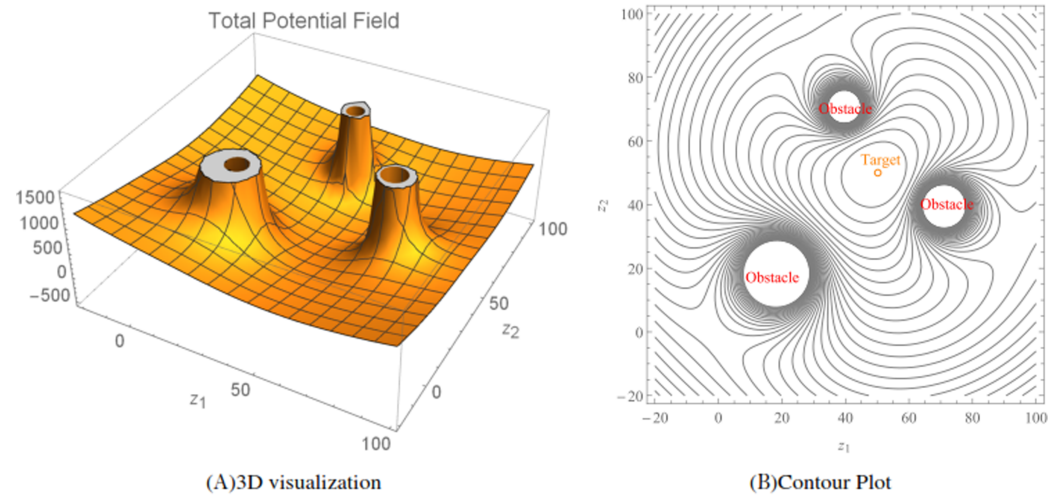
Figure 5 **The total potential fields and the corresponding contour plot generated using the Lyapunov function (15).** The radius of the obstacles were randomized between two and four, $r_w = 1$, $\alpha = 0.2$, β_k for $k = 1, 2$ and 3 were randomized between 50 and 70.

This auxiliary function will be multiplied to the total repulsive potential.

A Lyapunov function

Using the attractive and repulsive potentials with the auxiliary function, a total potential called the Lyapunov function, is formed as,

$$L(\mathbf{x}) = U_{att}(\mathbf{x}) + H(\mathbf{x})U_{rep}(\mathbf{x}). \tag{15}$$

An illustration of the total potentials for the Lyapunov function (15) for three randomly generated obstacles and a target situated at (50, 50) is shown in Fig. 5A, while Fig. 5B shows the corresponding contour plot generated over a workspace $-20 < z_1 < 100$ and $-20 < z_2 < 100$.

Velocity controllers

Along a trajectory of system (8),

$$\dot{L}(\mathbf{x}) = \nabla L(\mathbf{x})$$
$$= f(\mathbf{x})\dot{x} + g(\mathbf{x})\dot{y}, \tag{16}$$

where

$$f(\mathbf{x}) = (x - a)\left(\alpha + \sum_{k=1}^{q} \frac{\beta_k}{W_k(\mathbf{x})}\right) - \sum_{k=1}^{q} \beta_k \frac{H(\mathbf{x})}{W_k^2(\mathbf{x})}(x - o_{k1}) \tag{17}$$

and

$$g(\mathbf{x}) = (y - b)\left(\alpha + \sum_{k=1}^{q} \frac{\beta_k}{W_k(\mathbf{x})}\right) - \sum_{k=1}^{q} \beta_k \frac{H(\mathbf{x})}{W_k^2(\mathbf{x})}(y - o_{k2}). \tag{18}$$

Let there be scalars $\mu > 0$ and $\varphi > 0$. Then the velocity controllers of system (8) are

$$\rho = -\mu f(\mathbf{x}) \text{ and } \omega = -\varphi g(\mathbf{x}). \qquad (19)$$

ANGULAR VELOCITIES AND THEIR LIMITATIONS

The system of ODEs (6) is substituted into the time derivative of (15) as shown below:

$$
\begin{aligned}
\dot{L}(\mathbf{x}) &= f(\mathbf{x}) \cdot \dot{x} + g(\mathbf{x}) \cdot \dot{y} \\
&= \frac{rf(\mathbf{x})}{\zeta} \left(v_R \left(\frac{\zeta}{2} \cos\theta - \eta \sin\theta \right) + v_L \left(\frac{\zeta}{2} \cos\theta + \eta \sin\theta \right) \right) \\
&\quad + \frac{rg(\mathbf{x})}{\zeta} \left(v_R \left(\frac{\zeta}{2} \sin\theta + \eta \cos\theta \right) + v_L \left(\frac{\zeta}{2} \sin\theta - \eta \cos\theta \right) \right) \\
&= \frac{r}{\zeta} \left(f(\mathbf{x}) \left(\frac{\zeta}{2} \cos\theta - \eta \sin\theta \right) + g(\mathbf{x}) \left(\frac{\zeta}{2} \sin\theta + \eta \cos\theta \right) \right) v_R \\
&\quad + \frac{r}{\zeta} \left(f(\mathbf{x}) \left(\frac{\zeta}{2} \cos\theta + \eta \sin\theta \right) + g(\mathbf{x}) \left(\frac{\zeta}{2} \sin\theta - \eta \cos\theta \right) \right) v_L.
\end{aligned}
$$

Subsequently, angular velocities of the rear right and left wheels could be defined as

$$
\left.
\begin{aligned}
v_R &:= -\frac{\kappa_1 r}{\zeta} \left(f(\mathbf{x}) \left(\frac{\zeta}{2} \cos\theta - \eta \sin\theta \right) + g(\mathbf{x}) \left(\frac{\zeta}{2} \sin\theta + \eta \cos\theta \right) \right), \\
v_L &:= -\frac{\kappa_2 r}{\zeta} \left(f(\mathbf{x}) \left(\frac{\zeta}{2} \cos\theta + \eta \sin\theta \right) + g(\mathbf{x}) \left(\frac{\zeta}{2} \sin\theta - \eta \cos\theta \right) \right),
\end{aligned}
\right\} \qquad (20)
$$

where κ_1 and κ_2 are desired to be some arbitrary continuous positive function of x and y, and $f(\mathbf{x})$ and $g(\mathbf{x})$ are defined in (17) and (18), respectively. Moreover, the angular velocities of the rear right and left wheels do have restrictions practically. An illustration of this restriction is shown in Fig. 6. To add on, maximum angular velocities of the left and right wheels of the wheelchair can also be treated as artificial constraints which could be part of the total potential as repulsive potentials. However, the equivalent is to bound the angular velocities. The later is discussed in this paper.

The functions $\kappa_1 = \kappa_1(x, y) > 0$ and $\kappa_2 = \kappa_2(x, y) > 0$ lay an important role in restricting the sizes of v_R and v_L, respectively. Given $\chi > 0$ from (20),

$$
\left.
\begin{aligned}
|v_R| &\leq \kappa_1 \left(\frac{r}{2} + \frac{r\eta}{\zeta} \right) (\chi + |f(\mathbf{x})| + |g(\mathbf{x})|), \\
|v_L| &\leq \kappa_2 \left(\frac{r}{2} + \frac{r\eta}{\zeta} \right) (\chi + |f(\mathbf{x})| + |g(\mathbf{x})|).
\end{aligned}
\right\} \qquad (21)
$$

If we let $v_{Rmax} := \max|v_R|$ and $v_{Lmax} := \max|v_L|$ be the maximum angular velocities then from (21)

$$\kappa_1 := \frac{v_{Rmax}}{\left(\frac{r}{2} + \frac{r\eta}{\zeta} \right) (\chi + |f(\mathbf{x})| + |g(\mathbf{x})|)} \qquad (22)$$

and
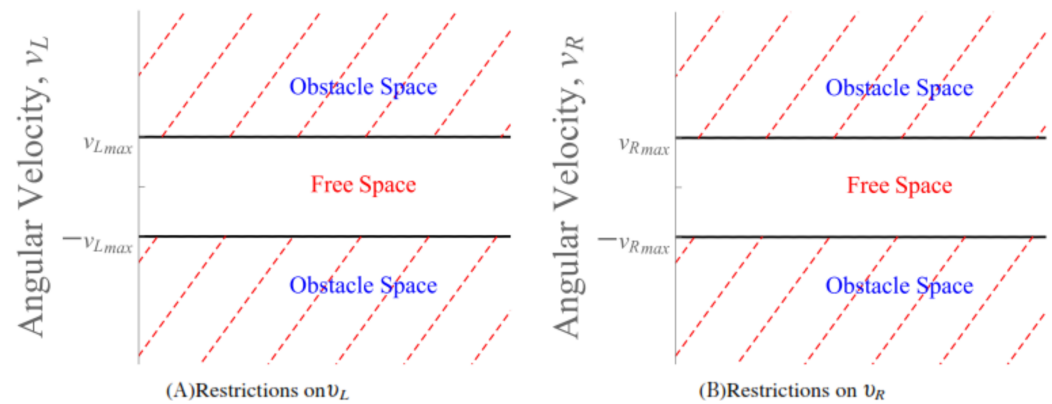
Figure 6 The obstacle space forms the artificial constraints that restricts the angular velocities υ_L and υ_R.

$$\kappa_2 := \frac{\upsilon_{Lmax}}{\left(\dfrac{r}{2} + \dfrac{r\eta}{\zeta}\right)(\chi + |f(\mathbf{x})| + |g(\mathbf{x})|)}. \tag{23}$$

STABILITY ANALYSIS

It is evident that $L(\mathbf{x})$, is positive over the domain

$$D(L(\mathbf{x})) := \{\mathbf{x} \in \mathbb{R}^{2n} : W_k(\mathbf{x}) > 0, \ \forall k = \{1, 2, 3, \ldots, q\}\}$$

and with respect to system (6) and the angular velocities of the rear right and left wheels mentioned in (20),

$$\dot{L}(\mathbf{x}) = -\left(\frac{\upsilon_R^2}{\kappa_1} + \frac{\upsilon_L^2}{\kappa_2}\right) \leq 0.$$

$\forall \mathbf{x} \in D(L(\mathbf{x}))$. At the target, where $(x, y) = (a, b)$, the angular velocities, υ_R and υ_L, are zero because $f(\mathbf{x}) = 0$ and $g(\mathbf{x}) = 0$. It is easy to see that $L(\mathbf{x}_e) = 0, L(\mathbf{x}) > 0 \ \forall \ \mathbf{x} \neq \mathbf{x}_e$ and $\dot{L}(\mathbf{x}) \leq 0$. Therefore, system (6) is stable.

SIMULATION RESULTS

Simulations were generated using the Wolfram Mathematica 11.2 software. To achieve the desired results a number of sequential Mathematica commands were executed. System (6) was numerically simulated using RK4 method (Runge–Kutta Method). Due to the inherent nature of the artificial potential field method, which includes LbCS, there is a possibility that some initial conditions can produce trajectories that get trapped in local minima. Firstly, the initial position of the robot relative to the obstacle. For instance, if the robot is near the obstacle then there is a possibility that the robot will move into local minima and get trapped there. Secondly, there is a need to avoid the collinear situation of the robot's initial position, obstacle position, and target location (*Vanualailai,*

Table 1 Example 1. Numerical values of the initial states, constraints, and control and convergence parameters of the wheelchair robot.

Initial configuration	
Rectangular position	$(x_0, y_0) = (10, 10)$
Initial orientation, θ rad	Randomly generated
Constraints	
Dimensions	$\zeta = 5, r = 2, \eta = 3$
Target	$(a, b) = (100, 100)$
Fixed obstacle	$(o_{11}, o_{12}) = (50, 50)$
Radius of fixed obstacle	$r_{o1} = 10$
Maximum angular velocities	$\upsilon_{Rmax} = \upsilon_{Lmax} = 1$
Parameter used to bound υ_R and υ_L	$\chi = 1$
Control parameters	
Target convergence	$\alpha = 2$
Obstacle avoidance	$\beta_1 = 0.01$

Sharma & Nakagiri, 2008). Such initial conditions are avoided when assigning values to parameters through brute-force.

Example 1. The wheelchair robot has to maneuver to its target avoiding the obstacle in its way. For this example, Table 1 shows the numerical values of the initial states, constraints, and control and convergence parameters used for the wheelchair. As time evolves the robot moves to its target as shown in Fig. 7. Figure 8 shows the evolution of the monotonically decreasing $L(\mathbf{x})$ and its time derivative. This indicates that the wheelchair robot is converging to its target. The angular velocities, υ_R and υ_L of the wheelchair robot is shown in Fig. 9. The negative angular velocities of the wheels indicate that the wheels are turned in the reverse direction and there is rapid deceleration wheelchair robot approaches the target. The linear velocities of the right and left wheels of the wheelchair robot is shown in Fig. 10. In Fig. 11 snapshots had been taken which shows the rotational motion of the wheelchair robot.

Example 2. Five static obstacles were randomly generated, and the wheelchair robot has to avoid those that fall on its path in its way to its target. Table 2 only shows the numerical values of the initial states, constraints, and control and convergence parameters of the wheelchair robot which were different from *Example 1* for this example. The position at different times of wheelchair robot as it maneuvers to its target avoiding the obstacles in its way is shown in Fig. 12. The angular velocities, υ_R and υ_L of the wheelchair robot is shown in Fig. 13. The negative velocities of the wheels indicate that the wheels are turned in the reverse direction and there is rapid deceleration wheelchair robot approaches the target. The evolution of $L(\mathbf{x})$ and its time derivative are similar to that of *Example 1*. Monotonically decreasing $L(\mathbf{x})$ indicates that the wheelchair robot is converging to its target.

Example 3. Five random obstacles were generated in the workspace of the wheelchair robot. The robot has to maneuver to its target avoiding the obstacle in its way. For this example, Table 2 shows the numerical values of the initial states, and constraints.
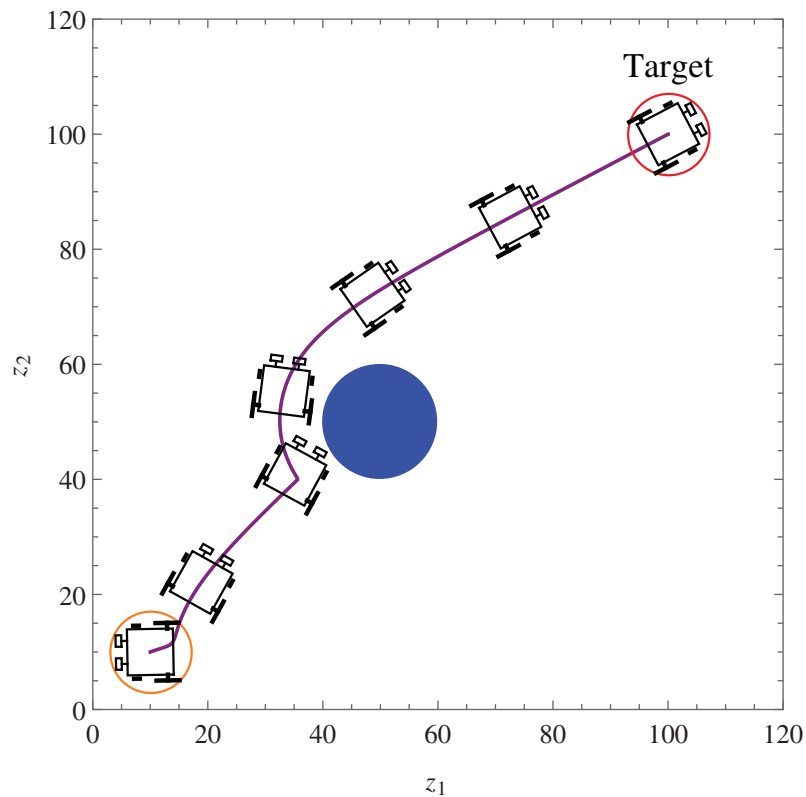
Figure 7 Example 1. Position and orientation of the wheelchair robot at $t = 0, 27, 39, 78, 95, 115$ and 140 respectively. The trajectory of (x, y) is shown in solid line.
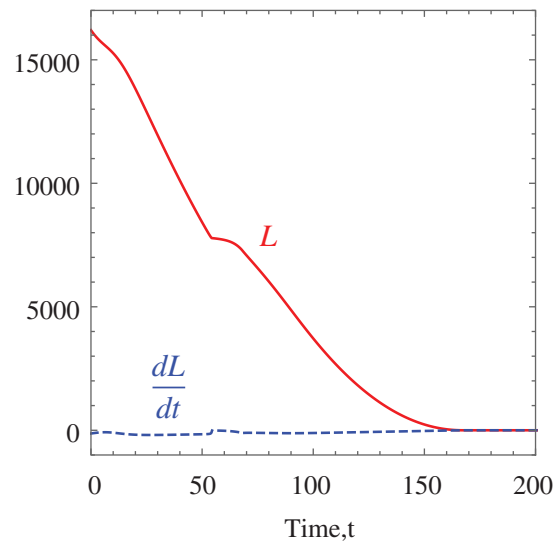
Figure 8 Example 1. Monotonically decreasing Lyapunov function and its time derivative.

The control parameter for target convergence is 0.1 whereas the obstacle avoidance parameter was randomised between 3 and 10. As time evolves the robot moves to its target as shown in Fig. 14. Figure 15 shows the evolution of the monotonically decreasing $L(\mathbf{x})$
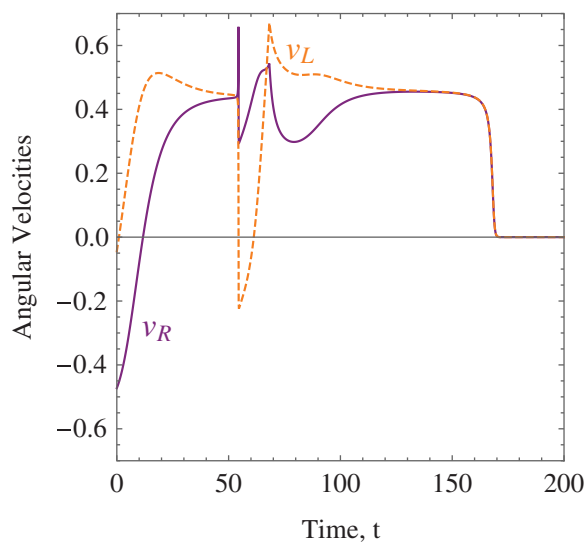
Figure 9 *Example 1.* The angular velocities of the wheelchair robot showing rapid deceleration as it approaches the target.
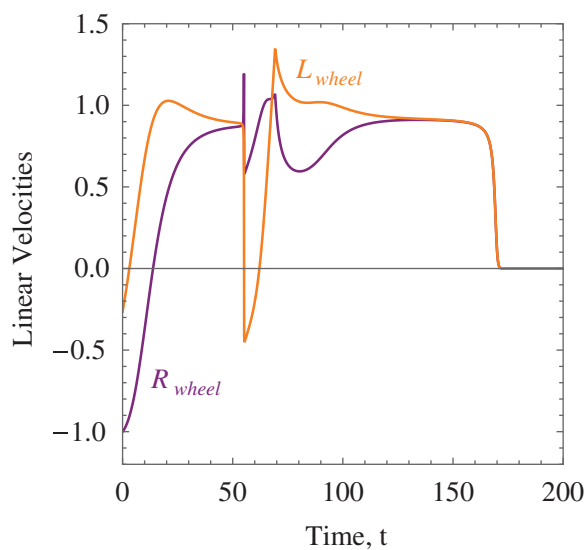
Figure 10 *Example 1.* The linear velocities of the wheels of the wheelchair robot showing rapid deceleration as it approaches the target.

and its time derivative. This indicates that the wheelchair robot is converging to its target. The angular velocities, v_R and v_L of the wheelchair robot is shown in Fig. 16. The negative velocities of the wheels indicate that the wheels are turned in the reverse direction and there is rapid deceleration wheelchair robot approaches the target.

DISCUSSION

The introduction of smart wheelchairs is making our society socially and economically inclusive for PWDs. In this paper, a set of nonlinear, time-invariant, continuous, and stabilizing velocity controllers of a wheelchair robot has been established to navigate in an
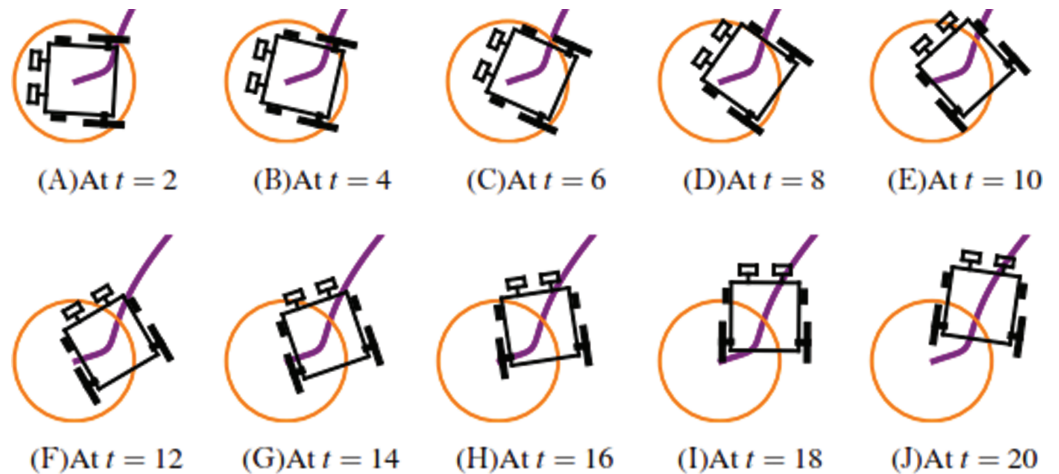
Figure 11 Example 1. Images taken at t = 2, 4, 6, 8, 10, 12, 14, 16, 18 and 20 respectively showing the rotational motion of the wheelchair robot.

Table 2 Example 2. Numerical values of the initial states, constraints, and control and convergence parameters of the wheelchair robot.

Initial configuration	
Rectangular position	(x_0, y_0) = (110, 10)
Constraints	
Target	(a, b) = (10, 100)
Fixed obstacles	Five were (q = 5) randomly generated
Radius of fixed obstacle	Randomized between 2 and 10
Obstacle avoidance	β_k = 0.001 for k = 1, 2, 3, …, q
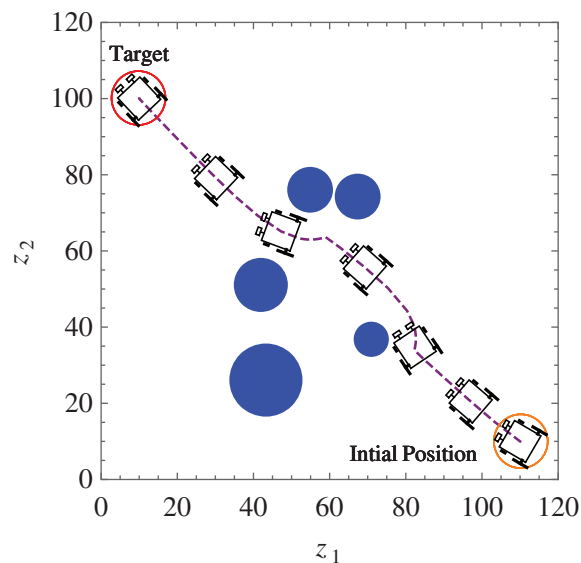
Figure 12 Example 2. Position and orientation of the wheelchair robot at t = 0, 2, 8, 19, 31, 34 and 50 respectively. The trajectory of (x, y) is shown in dashed line.
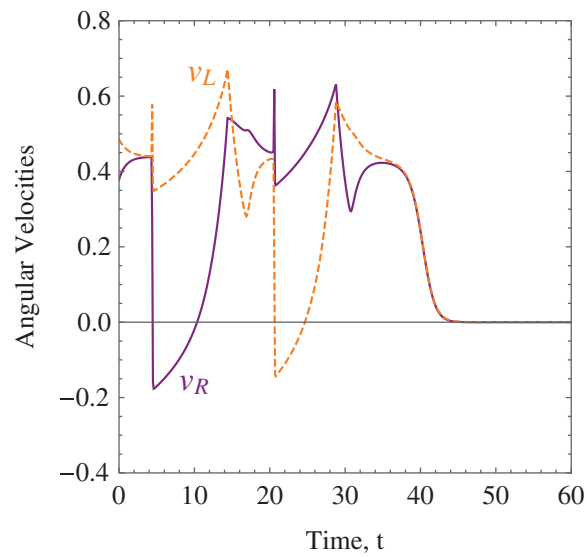
Figure 13 *Example 2.* The angular velocities of the wheelchair robot showing rapid deceleration as it approaches the target.
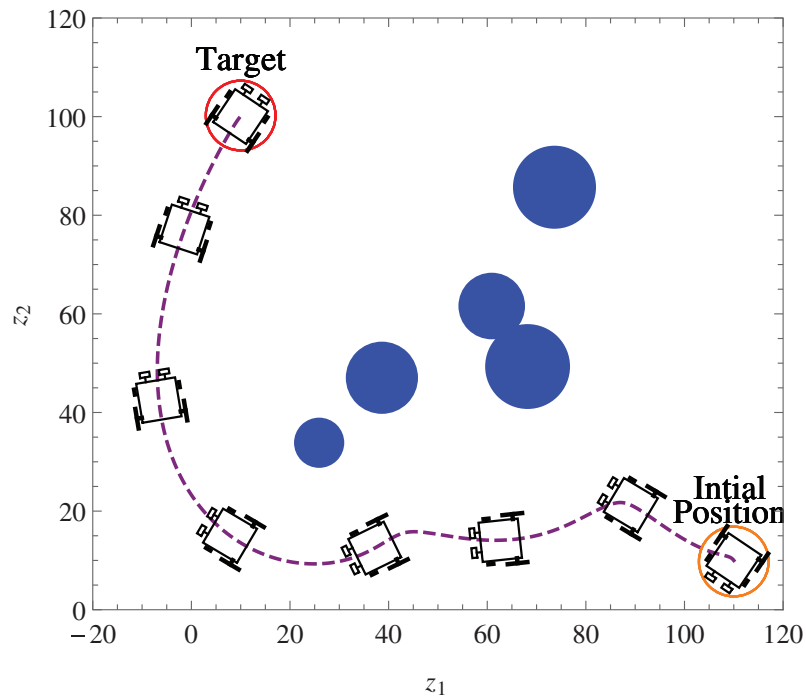
Figure 14 *Example 3.* Position and orientation of the wheelchair robot at $t = 0$, 45, 95, 140, 190, 230, 270 and 360 respectively. The trajectory of (x, y) is shown in dashed line.

obstacle-ridden environment while observing system restrictions and limitations. Simulation results such as the ones shown in Figs. 7, 12, and 14 show the controllers' effectiveness and system robustness for navigation in an obstacle-ridden environment.
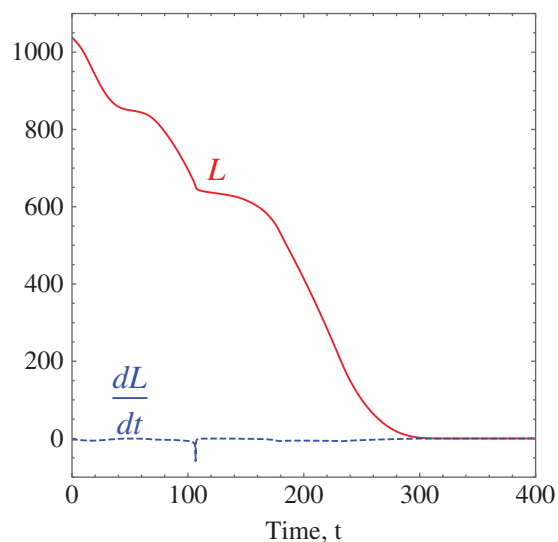
Figure 15 *Example 3*. Monotonically decreasing Lyapunov function and its time derivative.
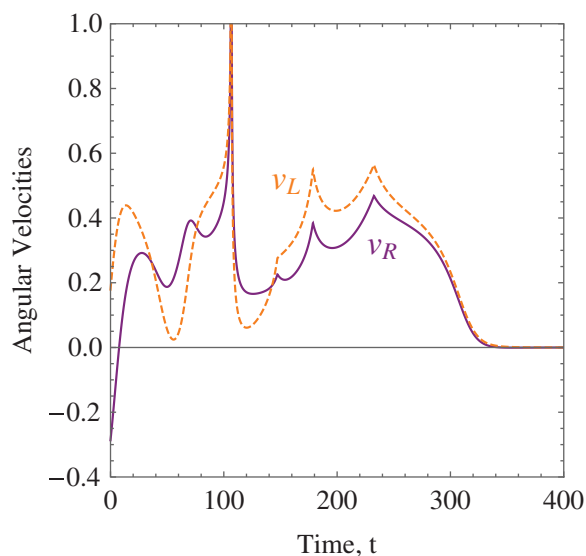
Figure 16 *Example 3*. The angular velocities of the wheelchair robot showing rapid deceleration as it approaches the target.

This has provided a solution to the common problem tagged to wheelchairs that require human interactions whereby persons with special disabilities are incapable of any interactions or are not able to provide any commands to the wheelchairs. For instance, for those who have severe paralysis, mental impairment, concomitant impairments, musculoskeletal problems, and spinal cord injury patients, even the simplest of the tasks requiring moving from one place to the other are being compromised. When we look at the smart wheelchair proposed in this paper, this problem is resolved where the person using the wheelchair is not required to provide any command, and navigation or the task can be controlled centrally. The system proposed suits a user's routine activities, which

could be pre-programmed as the central command. For instance, at a specific time, the user should be heading for the dining area, washroom, tea room, and so on, enabling the user to move around for scheduled activities without assistance from another person. Whereas for ad-hoc activities, a user or another person (where the user is not capable) has to interact with the wheelchair to provide the command for navigation.

In comparison to the systems presented in *Borges et al. (2018)*, *Gulpanich, Petchhan & Wongvanich (2018)*, *Solea et al. (2015)*, *Saitoh, Takahashi & Konishi (2007)*, *Tomari, Kobayashi & Kuno (2014)*, *Xin et al. (2018)*, *Qin, Li & Nawaz (2018)*, *Yashoda et al. (2018)*, and *Shahnaz et al. (2017)* the current system is stable; shows system robustness, and most importantly, it navigates autonomously, whereas the systems presented in *Borges et al. (2018)*, *Gulpanich, Petchhan & Wongvanich (2018)*, *Solea et al. (2015)*, *Saitoh, Takahashi & Konishi (2007)*, *Tomari, Kobayashi & Kuno (2014)*, *Xin et al. (2018)*, *Qin, Li & Nawaz (2018)*, *Yashoda et al. (2018)*, and *Shahnaz et al. (2017)* require user interaction. However, the major drawback of LbCS based on the classical approach of artificial potential field technique is the algorithm singularities or local minima. To add on, the sharp change in angular velocities of the wheels is a limitation of this study as well. Fine-tuning the control parameters would minimize the sharp change of velocities of the two wheels to a certain extend. However, to ensure that there is no sharp change in velocities of the wheels, there is a need to mathematically optimize the tuning parameters, which is an open field of study.

CONCLUSION

Stabilizing two-dimensional velocity-based controllers were proposed for two rear wheels driven nonholonomic wheelchair with two front castor wheels. The nonlinear time-invariant continuous controllers enabled the wheelchair, governed by its kinematic equations, to navigate from its initial configuration to a target location in an obstacle-ridden environment while observing the system restrictions and limitations. Interaction of the three main pillars of LbCS, which are safety, shortness, and smoothest path for motion planning, bring about cost and time effectiveness and efficiency of the velocity controllers. From the authors' point of view, this is the first time such stabilizing continuous velocity-based controllers are derived for autonomous wheelchairs in Lyapunov's sense.

This paper is a theoretical exposition into the applicability of LbCS, and we have restricted ourselves to showing the effectiveness of velocity-based control laws using computer-based simulations of interesting scenarios and numerical proofs. The drawback of this approach is that algorithm singularities (local minima) can be introduced. In practical applications, continuity has to be discretized, and only asymptotic stability could be shown. It is feasible for the industry sector to include such controllers for the development of autonomous wheelchairs. The development of such assistive technologies, which are affordable, can accelerate PWD's social and economic inclusion.

The future work will consider combining the current algorithm, however, with acceleration controllers to one of the heuristic-based approaches to form a hybrid system, which inherits the benefits of LbCS but can flush out local minima using the latter

approach. The acceleration controllers will increase the comfort level of the user of the wheelchair. Furthermore, motion planning and formation control of multiple nonholonomic wheelchairs for real-like applications will also be considered.

ACKNOWLEDGEMENTS

The authors would like to acknowledge Dr. Bibhya Sharma who is an Associate Professor of Mathematics in the School of Information Technology, Engineering, Mathematics and Physics of The University of the South Pacific for his comments which led to the enhancement of the quality and presentation of this article.

Funding

The authors received no funding for this work.

Competing Interests

The authors declare that they have no competing interests.

Author Contributions

- Sandeep Ameet Kumar conceived and designed the experiments, performed the experiments, analyzed the data, performed the computation work, prepared figures and/ or tables, authored or reviewed drafts of the paper, and approved the final draft.
- Jito Vanualailai analyzed the data, authored or reviewed drafts of the paper, reviewing and editing, and approved the final draft.
- Avinesh Prasad performed the computation work, authored or reviewed drafts of the paper, reviewing and editing, and approved the final draft.

Data Availability

   The code is available in the Supplemental File.

Supplemental Information

Supplemental information for this article can be found online at http://dx.doi.org/10.7717/peerj-cs.725#supplemental-information.

REFERENCES

Andaluz VH, Canseco P, Varela J, Ortiz JS, Peˊrez MG, Morales V, Robertˊ1 F, Carelli R. 2015. Modeling and control of a wheelchair considering center of mass lateral displacements. *Intelligent Robotics and Applications. Lecture Notes in Computer Science* **9246**:254–270 DOI 10.1007/978-3-319-22873-0.

Assaf M, Kumar R, Nambiar K, Narayan S, Nath N, Reddy Y, Sharma K, Sharma B. 2018. Enabling students with severe disabilities to communicate with learning environments. In: *2018 5th Asia-Pacific World Congress on Computer Science and Engineering (APWC on CSE).* 201–206.

Bharath R, Sreenidhi DR, Tarun S. 2018. Design and implementation of robotic wheelchair. In: *2018 10th International Conference on Communication Systems Networks (COMSNETS).* 528–530.

Borges B, Chandra A, Kalantri R, Gupta S, Dsilva G, Rajguru S. 2018. Android controlled wheelchair. In: *2018 First International Conference on Secure Cyber Computing and Communication (ICSCCC).* 1–7.

Bumuller A, Skerl K. 2018. Development of a modular smart wheelchair. In: *2018 International IEEE Conference and Workshop in Óbuda on Electrical and Power Engineering (CANDO-EPE).* Piscataway: IEEE, 49–54.

Chand V, Prasad A, Chaudhary K, Sharma B, Chand S. 2020. A face-off-classical and heuristic-based path planning approaches. In: *2020 IEEE Asia-Pacific Conference on Computer Science and Data Engineering (CSDE).* Piscataway: IEEE, 1–6.

Chen X, Chase JG, Wolm P, Anstis I, Oldridge J, Hanbury-Webber W, Elliot R, Pettigrew W. 2008. System identification and modelling of front wheel drive electric wheelchairs. *IFAC Proceedings Volumes* **41(2)**:3076–3081 DOI 10.3182/20080706-5-KR-1001.00522.

Chen L, Wang S, Hu H, Gu D, Dukes I. 2008. Chapter 17-voice-directed autonomous navigation of a smart-wheelchair. In: Diez P, ed. *Smart Wheelchairs and Brain-Computer Interfaces.* Cambridge: Academic Press, 405–424.

Darweesh H, Takeuchi E, Takeda K, Ninomiya Y, Sujiwo A, Morales LY, Akai N, Tomizawa T, Kato S. 2017. Open source integrated planner for autonomous navigation in highly dynamic environments. *Journal of Robotics and Mechatronics* **29(4)**:668–684 DOI 10.20965/jrm.2017.p0668.

Devi A, Vanualailai J, Kumar SA, Sharma B. 2017. A cohesive and well-spaced swarm with application to unmanned aerial vehicles. In: *Proceedings of the 2015 2017 International Conference on Unmanned Aircraft Systems (ICUAS).* Miami, FL, USA. Piscataway: IEEE, 698–705.

Dhaouadi R, Hatab AA. 2013. Dynamic modelling of differential-drive mobile robots using Lagrange and Newton–Euler methodologies: a unified framework. In: *ICRA 2013.*

Eid MA, Giakoumidis N, Saddik AEl. 2016. A novel eye-gaze-controlled wheelchair system for navigating unknown environments: case study with a person with ALS. *IEEE Access* **4**:558–573 DOI 10.1109/ACCESS.2016.2520093.

Gillham M, Howells G. 2015. A dynamic localized adjustable force field method for real-time assistive non-holonomic mobile robotics. *International Journal of Advanced Robotic Systems* **2015(10)**:1–21 DOI 10.5772/61190.

Gulati S, Kuipers B. 2008. High performance control for graceful motion of an intelligent wheelchair. In: *2008 IEEE International Conference on Robotics and Automation.* Piscataway: IEEE, 3932–3938.

Gulpanich S, Petchhan J, Wongvanich N. 2018. plc. In: *57th Annual Conference of the Society of Instrument and Control Engineers of Japan (SICE).*

Hartman A, Nandikolla VK. 2019. Human-machine interface for a smart wheelchair. *Journal of Robotics* **2019(3)**:1–16 DOI 10.1155/2019/4837058.

Herrera D, Roberti F, Carelli R, Andaluz V, Varela J, Ortiz J, Canseco P. 2018. Modeling and path-following control of a wheelchair in human-shared environments. *International Journal of Humanoid Robotics* **15(2)**:1850010 DOI 10.1142/S021984361850010X.

Kumar SA, Sharma B, Vanualailai J, Prasad A. 2021a. Stable switched controllers for a swarm of UGVs for hierarchal landmark navigation. *Swarm and Evolutionary Computation* **65(4)**:100926 DOI 10.1016/j.swevo.2021.100926.

Kumar SA, Vanualailai J. 2017. A Lagrangian UAV swarm formation suitable for monitoring exclusive economic zone and for search and rescue. In: *Proceedings of the 2017 IEEE Conference on Control Technology and Applications, Kohala Coast, Hawai'i, USA*. Piscataway: IEEE, 1874–1879.

Kumar SA, Vanualailai J, Sharma B. 2015a. Lyapunov functions for a planar swarm model with application to nonholonomic planar vehicles. In: *Proceedings of the 2015 IEEE Conference on Control Applications*. Sydney, Australia. Piscataway: IEEE, 1919–1924.

Kumar SA, Vanualailai J, Sharma B. 2015b. Lyapunov-based control for a swarm of planar nonholo- nomic vehicles. *Mathematics in Computer Science* **9(4)**:461–475 DOI 10.1007/s11786-015-0243-z.

Kumar SA, Vanualailai J, Sharma B, Chaudary A, Kapadia V. 2016. Emergent formations of a Lagrangian swarm of unmanned ground vehicles. In: *Proceedings of the 2016 14th International Conference on Control, Automation, Robotics and Vision, ICARCV 2016*. Phuket, Thailand. Piscataway: IEEE.

Kumar SA, Vanualailai J, Sharma B, Prasad A. 2021b. Velocity controllers for a swarm of unmanned aerial vehicles. *Journal of Industrial Information Integration* **22(1)**:100198 DOI 10.1016/j.jii.2020.100198.

Lazarowska A. 2019. Discrete artificial potential field approach to mobile robot path planning. *IFAC-PapersOnLine* **52(8)**:277–282 DOI 10.1016/j.ifacol.2019.08.083.

Maule L, Fornaser A, Leuci M, Conci N, Da Lio M, De Cecco M. 2016. Development of innovative HMI strategies for eye controlled wheelchairs in virtual reality. In: De Paolis LT, Mongelli A, eds. *Augmented Reality, Virtual Reality, and Computer Graphics*. Cham: Springer International Publishing, 358–377.

Moon N, Baker P, Goughnour K. 2019. Designing wearable technologies for users with disabilities: accessibility, usability, and connectivity factors. *Journal of Rehabilitation and Assistive Technologies Engineering* **6**:1–12 DOI 10.1177/2055668319862137.

Ng DW-K, Goh SY. 2020. Indirect control of an autonomous wheelchair using SSVEP BCI. *Journal of Robotics and Mechatronics* **32(4)**:761–767 DOI 10.20965/jrm.2020.p0761.

Prasad A, Sharma B, Vanualailai J, Kumar SA. 2020. A geometric approach to target convergence and obstacle avoidance of a nonstandard tractor-trailer robot. *International Journal of Robust and Nonlinear Control* **30(13)**:4924–4943 DOI 10.1002/rnc.5021.

Prasad A, Sharma B, Vanualailai J, Kumar S. 2021. Motion control of an articulated mobile manipulator in 3d using the lyapunov-based control scheme. Epub ahead of print 30 April 2021. *International Journal of Control* DOI 10.1080/00207179.2021.1919927.

Qin F, Li J, Nawaz SA. 2018. Design and implementation of automkatic following wheelchair. In: *2018 IEEE International Conference on Advanced Manufacturing (ICAM)*. Piscataway: IEEE, 403–406.

Raghuwaiya K, Sharma B, Vanualailai J. 2018. Leader-follower based locally rigid formation control. *Journal of Advanced Transportation* **2018(5)**:1–14 DOI 10.1155/2018/5278565.

Rösmann C, Hoffmann F, Bertram T. 2017. Integrated online trajectory planning and optimization in distinctive topologies. *Robotics and Autonomous Systems* **88(6)**:142–153 DOI 10.1016/j.robot.2016.11.007.

Saitoh T, Takahashi N, Konishi R. 2007. Oral motion controlled intelligent wheelchair. In: *SICE Annual Conference 2007*. 341–346.

Shahnaz C, Maksud A, Fattah SA, Chowdhury SS. 2017. Low-cost smart electric wheelchair with destination mapping and intelligent control features. In: *2017 IEEE International Symposium on Technology and Society (ISTAS)*. Piscataway: IEEE, 1–6.

Sharma B, Raj J, Vanualailai J. 2018. Navigation of carlike robots in an extended dynamic environment with swarm avoidance. *International Journal of Robust and Nonlinear Control* **28(2)**:678–698 DOI 10.1002/rnc.3895.

Sharma B, Singh S, Vanualailai J, Prasad A. 2018. Globally rigid formation of n-link doubly nonholonomic mobile manipulators. *Robotics and Autonomous Systems* **2018(3)**:69–84 DOI 10.1016/j.robot.2018.02.006.

Sharma B, Vanualailai J, Prasad A. 2011. Formation control of a swarm of mobile manipulators. *Rocky Mountain Journal of Mathematics* **41(3)**:900–940 DOI 10.1216/RMJ-2011-41-3-909.

Sharma B, Vanualailai J, Prasad A. 2017. A dϕ-strategy: facilitating dual-formation control of a virtually connected team. *Journal of Advanced Transportation* **2017**:1–17.

Sharma B, Vanualailai J, Singh S. 2012. Lyapunov-based nonlinear controllers for obstacle avoidance with a planar n-link doubly nonholonomic manipulator. *Robotics and Autonomous Systems* **60(12)**:1484–1497 DOI 10.1016/j.robot.2012.07.014.

Sharma B, Vanualailai J, Singh S. 2014. Tunnel passing maneuvers of prescribed formations. *International Journal of Robust and Nonlinear Control* **24(5)**:876–901.

Sharma B, Vanualailai J, Singh S. 2015. Motion planning and posture control of multiple n-link doubly nonholonomic manipulators. *Robotica* **35**:1–25.

Solea R, Filipescu A, Filipescu A, Minca E, Filipescu S. 2015. Wheelchair control and navigation based on kinematic model and iris movement. In: *2015 IEEE 7th International Conference on Cybernetics and Intelligent Systems (CIS) and IEEE Conference on Robotics, Automation and Mechatronics (RAM)*. Piscataway: IEEE, 78–83.

Takahashi I, Murakami T. 2018. Fall prevention and vibration suppression of wheelchair using rider motion state. In: *2018 International Power Electronics Conference (IPEC-Niigata 2018-ECCE Asia)*. 575–582.

Tomari MRM, Kobayashi Y, Kuno Y. 2012. Development of smart wheelchair system for a user with severe motor impairment. *Procedia Engineering* **41**:538–546 DOI 10.1016/j.proeng.2012.07.209.

Tomari R, Kobayashi Y, Kuno Y. 2014. Analysis of socially acceptable smart wheelchair navigation based on head cue information. *Procedia Computer Science* **42(4)**:198–205 DOI 10.1016/j.procs.2014.11.052.

Utkal M, Mohammed A, Shivneel K. 2017. Smart path guidance mobile aid for visually disabled per-sons. *Procedia Computer Science* **105**:52–56.

Vanualailai J, Sharma B, Nakagiri S. 2008. An asymptotically stable collision-avoidance system. *International Journal of Non-Linear Mechanics* **43(9)**:925–932 DOI 10.1016/j.ijnonlinmec.2008.06.012.

Xin L, Gao S, Tang J, Xu X. 2018. Design of a brain controlled wheelchair. In: *2018 IEEE 4th International Conference on Control Science and Systems Engineering (ICCSSE)*. Piscataway: IEEE, 112–116.

Yashoda HGMT, Piumal AMS, Polgahapitiya PGSP, Mubeen MMM, Muthugala MAVJ, Jayasekara AGBP. 2018. Design and development of a smart wheelchair with multiple control interfaces. In: *2018 Moratuwa Engineering Research Conference (MERCon)*. 324–329.